

## Experiment Report Form

**The double page inside this form is to be filled in by all users or groups of users who have had access to beam time for measurements at the ESRF.**

Once completed, the report should be submitted electronically to the User Office via the User Portal:

<https://www.esrf.fr/misapps/SMISWebClient/protected/welcome.do>

### ***Reports supporting requests for additional beam time***

Reports can be submitted independently of new proposals – it is necessary simply to indicate the number of the report(s) supporting a new proposal on the proposal form.

The Review Committees reserve the right to reject new proposals from groups who have not reported on the use of beam time allocated previously.

### ***Reports on experiments relating to long term projects***

Proposers awarded beam time for a long term project are required to submit an interim report at the end of each year, irrespective of the number of shifts of beam time they have used.

### ***Published papers***

All users must give proper credit to ESRF staff members and proper mention to ESRF facilities which were essential for the results described in any ensuing publication. Further, they are obliged to send to the Joint ESRF/ ILL library the complete reference and the abstract of all papers appearing in print, and resulting from the use of the ESRF.

Should you wish to make more general comments on the experiment, please note them on the User Evaluation Form, and send both the Report and the Evaluation Form to the User Office.

### **Deadlines for submission of Experimental Reports**

- 1st March for experiments carried out up until June of the previous year;
- 1st September for experiments carried out up until January of the same year.

### **Instructions for preparing your Report**

- fill in a separate form for each project or series of measurements.
- type your report, in English.
- include the reference number of the proposal to which the report refers.
- make sure that the text, tables and figures fit into the space available.
- if your work is published or is in press, you may prefer to paste in the abstract, and add full reference details. If the abstract is in a language other than English, please include an English translation.



	<b>Experiment title:</b> Synergism of microfocus X-ray and electron diffraction to elucidate structure-property relations in thermoelectric tellurides and clathrates	<b>Experiment number:</b> HS-4625
<b>Beamline:</b> ID11	<b>Date of experiment:</b> from: 05.10.2012 to: 09.10.2012	<b>Date of report:</b> 15.02.2014
<b>Shifts:</b> 12	<b>Local contact(s):</b> Loredana Erra	<i>Received at ESRF:</i>
<b>Names and affiliations of applicants (* indicates experimentalists):</b>  <b>Prof. Dr. Oliver Oeckler*</b> (Leipzig University / Ludwig Maximilian University, Munich) <b>M. Sc. Tobias Rosenthal*</b> (Ludwig Maximilian University, Munich) <b>M. Sc. Felix Fahrnbauer*</b> (Leipzig University) <b>B. Sc. Tilo Schmutzler*</b> (Leipzig University)		

## Report:

### Aim

In many cases, syntheses that involve quenching melts or high pressure conditions lead to samples that contain microcrystalline phases, often inhomogeneous but containing unknown and intriguing structures.<sup>[1]</sup> On the other hand, multinary systems with nanoscale heterostructures cannot be studied effectively by conventional X-ray experiments.<sup>[2]</sup> Such phases can easily be investigated by electron diffraction, but a detailed analysis of the atom arrangement is difficult due to dynamical diffraction. Electron crystallographic methods such as the automated diffraction tomography (ADT) can yield approximate structure models, but the interatomic distances, site occupancies and displacement parameters are rather imprecise. Suitable single-crystals on carbon-film-coated copper grids can be selected by means of selected-area electron diffraction (SAED) and X-ray spectroscopy (EDX). Datasets of such pre-selected crystallites obtained by a sub-micron synchrotron beam can be used to precisely refine approximate structure models from electron diffraction or to solve them *ab initio* and subsequently confirm them or analyze real-structure effects by transmission electron microscopy (TEM). The application of this method to nanostructured thermoelectric tellurides, disordered sulfides and zeolitic nitridophosphates not only yields answers to complex crystal-chemical questions, but also paves the way towards a profound understanding of structure-property relationships.

### Experiments and results

Despite the specific sample characteristics owing to a variety of preparation techniques, the general procedure for our experiments followed the same strategy. Prior to the beamtime, we examined each sample by means of TEM in combination with EDX in order to make absolutely sure to choose a crystallite of interest, i. e. a new compound or specific grains in heterostructures. We also acquired SEM images of the samples on carbon-film-coated TEM grids for the optical recovery of specific crystallites. The copper grids carrying the samples were fixed on glass fibers in a way that the crystal of choice (or parts of it) was best accessible by the beam. At beamline ID11, we used characteristic morphological features and the position of each sample on the grid for an approximate optical alignment and performed fluorescence scans to precisely re-locate the correct crystallites and to center them in the beam. For different groups of crystallites, the beamsize was gradually reduced from ca. 2x2  $\mu\text{m}$  to a sub-micron beam. The energy was kept at 42.1 keV, which guaranteed minimal absorption effects, a high flux of the brilliant beam at ID11 as well as high

resolution without moving the detector. We proved the efficiency and wide-range applicability of this procedure for different compounds from a variety of material classes:

**a)** In the first series of experiments, we analyzed metastable layered germanium antimony tellurides corresponding to the general formula  $\text{Ge}_{3+x}\text{Sb}_{2-x}\text{Te}_6$ . These phases (GST materials) belong to the most important class of phase-change materials and represent thermoelectrics with high figures of merit.<sup>[3]</sup> We collected complete datasets by focusing on single-crystalline parts of poorly crystalline material, which were pre-selected as described above. These compounds are characterized by rocksalt-type building blocks with van der Waals gaps between two anion layers. For  $x = 0$ , the structure adopts a trigonal structure type (space group  $R\bar{3}m$ ,  $a = 4.2756 \text{ \AA}$ ,  $c = 63.6201 \text{ \AA}$ ,  $R_{\text{int}} = 0.047$ ,  $R1 = 0.049$ ), similar to other GST compounds.<sup>[4]</sup>

**b)** Heterostructured materials such as  $[\text{CoSb}_2(\text{GeTe})_{0.5}](\text{GeTe})_{10.5}\text{Sb}_2\text{Te}_3$  are intriguing for thermoelectric applications as interfaces on the nanoscale are efficient phonon scattering centers and therefore reduce the thermal conductivity. Polished samples of  $(\text{GeTe})_{10.5}\text{Sb}_2\text{Te}_3$  as a matrix for nanoscale precipitates of skutterudite-type  $\text{CoSb}_2(\text{GeTe})_{0.5}$  were thinned with an Ar-ion beam. Suitable crystallites at the edge of the thinned section and the surrounding matrix were chosen by means of TEM and further analyzed using the sub-micron beam at ID11. The refinement of the matrix yielded cubic  $(\text{GeTe})_{10.5}(\text{Sb}_2\text{Te}_3)$  (space group  $Fm\bar{3}m$ ,  $a = 5.9890(7) \text{ \AA}$ ,  $R_{\text{int}} = 0.044$ ,  $R1 = 0.020$ , cf. Figure 1). Ge, Sb and vacancies are randomly distributed over the cation position, as it was shown for comparable materials.<sup>[4]</sup> The skutterudite-type precipitates (space group  $Im\bar{3}$ ,  $a = 8.91658(8) \text{ \AA}$ ,  $R_{\text{int}} = 0.0508$ ,  $R1 = 0.032$ ) show a pronounced distortion of the  $\text{Sb}_4$  units in the structure, which are nearly square for  $\text{CoSb}_3$ <sup>[5]</sup> and become increasingly distorted upon substitution by GeTe. No residual electron density was found in the voids, so in contrast to other (partially) filled skutterudites, substitution effects do not involve this position.

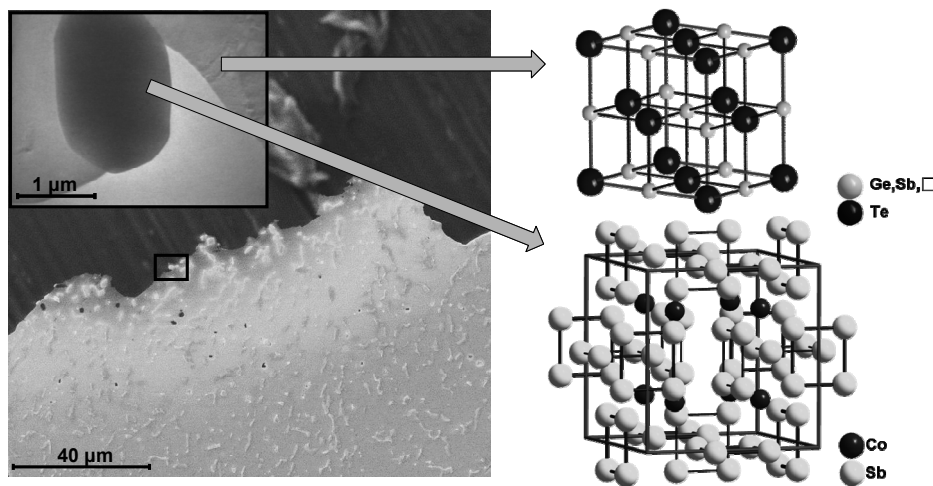


**Figure 1:** SEM image of a thinned sample of  $[\text{CoSb}_2(\text{GeTe})_{0.5}](\text{GeTe})_{10.5}\text{Sb}_2\text{Te}_3$  (left), examined skutterudite-type crystal and matrix region (TEM image, inset). Refined structures: GST matrix with rocksalt-type structure ( $R1 = 0.020$ , top right) and skutterudite-type precipitate ( $R1 = 0.032$ , bottom right).

**c)** For natural boulangierite minerals with the approximate composition  $\text{Pb}_5\text{Sb}_4\text{S}_{11}$ , cation ordering that results in monoclinic superstructures ( $P2_1/c$ ) was described. Higher orthorhombic symmetry ( $Pnma$ ) is found for synthetic samples and intermediates between these types were discussed, possibly co-existing within single crystals.<sup>[6]</sup> Yet, so far no satisfactory description of ordering phenomena and associated symmetry relationships has been given. We measured various synthetic samples, including additional robinsonite-type  $\text{Pb}_5\text{Sb}_6\text{S}_{14}$  ( $P\bar{1}$ ). We collected datasets at different spots along needle-like boulangierite-type crystallites. No long-range metal ordering could be verified, indicating that changes in symmetry within the single crystals do not occur on the examined scale. Multiple split positions for Sb derived from the synchrotron data are currently examined. These are most likely produced by a superposition of patterns of different short-range ordered structures. A standardized, comparable crystallographic setting of various structure models of ordered and disordered boulangierite-type structures given in the literature is also worked out.

**d)** Heterogeneous samples of quenched melts with the nominal composition “ $\text{Pb}_5\text{Sb}_4\text{S}_6\text{Te}_5$ ” contain small amounts of an unknown microcrystalline sulfide telluride with the composition  $\text{Pb}_8\text{Sb}_8\text{S}_{15}\text{Te}_5$  (which

was verified by TEM-EDX). SAED patterns indicated a tetragonal structure type, which was refined from high-quality ID11 synchrotron data obtained from the tip of one such crystallite (space group  $P4_1$ ,  $a = 8.0034(4) \text{ \AA}$ ,  $c = 15.0216(5) \text{ \AA}$ ,  $R_{\text{int}} = 0.040$ ,  $R1 = 0.037$ ). It is isostructural to  $\text{Ti}_3\text{PbCl}_5$  and consists of chains along [001] of distorted, single-side capped “heterocubane-like” units. The element distribution could be precisely refined, cations and anions are ordered in a way that bonds between neighboring chains are only formed through mixed cation positions (Pb/Sb = 19:1, 7:13 and 7:3) and “S-only” anion sites (cf. Figure 2). The structure model obtained is as precise as structure determinations by standard single-crystal methods using macroscopic crystals. Bond lengths are accurate, and the atom distribution could be confirmed by bond-valence calculations as well as by image-matching of simulations with high-resolution electron micrographs obtained of the same crystal that was examined at ID11.

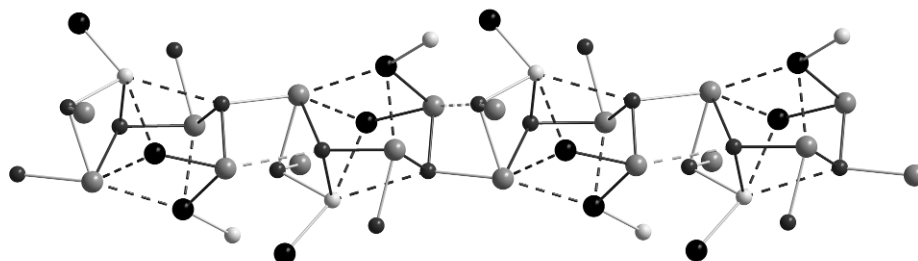


**Figure 2:** Structure of  $\text{Pb}_8\text{Sb}_8\text{S}_{15}\text{Te}_5$  (cutout of 3D network: characteristic chain along [001]), light gray: Sb, gray: Pb/Sb, dark gray: S, black: Te/S. Selected bonds are indicated as black lines, additional (longer) distances that complete the “heterocubane-like” units are given as dashed lines.

e) Rigid frameworks built up from  $\text{PN}_4$ ,  $\text{PON}_3$ ,  $\text{PO}_2\text{N}_2$  or  $\text{PO}_3\text{N}$  tetrahedra in (oxo)nitridophosphates exhibit, in principle, a large variety of structures and are, up to a certain extent, comparable to silicates. However, in contrast to the latter, only very few representatives of P/O/N compounds are known, some with clathrate or zeolitic structures.<sup>[7]</sup> By means of electron microscopy, two novel phases of Ca/Mg oxonitrodophosphates could be identified. Both were obtained as side-phases in high-pressure syntheses. The crystallite size is limited to a maximum of a few microns; however, the well crystallized areas are even smaller which makes the use of a microfocused synchrotron beam indispensable.  $(\text{Ca},\text{Mg})_2\text{PO}_3\text{N}$  adopts the orthorhombic  $\text{K}_2\text{SO}_4$  type (space group  $Pnma$ ,  $a = 6.8357(14) \text{ \AA}$ ,  $b = 5.5129(11) \text{ \AA}$ ,  $c = 9.4270(19) \text{ \AA}$ ,  $R_{\text{int}} = 0.043$ ,  $R1 = 0.049$ ) with two types of discrete  $\text{PO}_3\text{N}$  tetrahedra. One of the two Ca positions contains a small amount of Mg, which corresponds to the TEM-EDX results.  $(\text{Ca},\text{Mg})_7\text{P}_{18}\text{ON}_{34}$ , on the other hand, consists of a hexagonal network with channels of corner-sharing P/O/N tetrahedra and Ca/Mg ions for charge compensation (refined in space group  $P6_3/m$ ,  $a = 14.122(2) \text{ \AA}$ ,  $c = 8.1068(16) \text{ \AA}$ ,  $R_{\text{int}} = 0.133$ ,  $R1 = 0.120$ ). Both compounds may be phosphors for luminescence applications when doped with rare-earth atoms.

## Outlook

The combination of TEM and microfocus synchrotron diffraction is an excellent tool for challenging structure determinations where electron diffraction or (conventional as well as microfocused) X-ray diffraction alone are not sufficient. For the first time, the combination of both methods' advantages was successfully applied to a variety of material classes, making precise structure refinements of crystallites in heterogeneous microcrystalline samples possible. The first publications are already written, and several papers will follow soon. With the experience gained from this experiment, we will further optimize the procedure described, which should enable us to go to even more complex systems and experimental setups during our next beamtime.

- [1] a) S. C. Neumair, R. Kaindl, R.-D. Hoffmann, H. Huppertz, *Solid State Sci.* **2012**, *14*, 229; b) E. Mugnaioli, S. J. Sedlmaier, O. Oeckler, U. Kolb, W. Schnick, *Eur. J. Inorg. Chem.* **2012**, *1*, 121.
- [2] K. F. Hsu, S. Loo, F. Guo, W. Chen, J. S. Dyck, C. Uher, T. Hogan, E. K. Polychroniadis, M. G. Kanatzidis, *Science* **2004**, *303*, 818.
- [3] a) S. Raoux, D. Ielmini, M. Wuttig, I. Karpov, *Mrs. Bull.* **2012**, *37*, 118; b) S. Raoux, *Annu. Rev. Mater. Res.* **2009**, *39*, 25; c) T. Rosenthal, M. N. Schneider, C. Stiewe, M. Döblinger, O. Oeckler, *Chem. Mater.* **2011**, *23*, 4349.
- [4] M. N. Schneider, F. Fahrnbauer, T. Rosenthal, M. Döblinger, C. Stiewe, O. Oeckler, *Chem. Eur. J.* **2012**, *18*, 1209.
- [5] J. R. Sootsman, D. Y. Chung, M. G. Kanatzidis, *Angew. Chem. Int. Ed.* **2009**, *48*, 8616.
- [6] a) L. Born, E. Hellner, *Amer. Mineral.* **1960**, *45*, 1266; b) K. Bente, R. Anton, *Mineral. Petrol.* **1995**, *53*, 209.
- [7] a) S. Correll, O. Oeckler, N. Stock, W. Schnick, *Angew. Chem. Int. Ed.* **2003**, *42*, 3549; b) D. Baumann, S. J. Sedlmaier, W. Schnick, *Angew. Chem. Int. Ed.* **2012**, *51*, 4707; c) F. Karau, W. Schnick, *Angew. Chem. Int. Ed.* **2006**, *45*, 4505.